Strain-tunable band parameters of ZnO monolayer in graphene-like honeycomb structure

Harihar Behera* and Gautam Mukhopadhyay†

Department of Physics, Indian Institute of Technology, Powai, Mumbai-400076, India

Abstract

We present ab initio calculations which show that the direct-band-gap, effective masses and Fermi velocities of charge carriers in ZnO monolayer (ML-ZnO) in graphene-like honeycomb structure are all tunable by application of in-plane homogeneous biaxial strain. Within our simulated strain limit of ±10%, the band gap remains direct and shows a strong non-linear variation with strain. Moreover, the average Fermi velocity of electrons in unstrained ML-ZnO is of the same order of magnitude as that in graphene. The results promise potential applications of ML-ZnO in mechatronics/straintronics and other nano-devices such as the nano-electromechanical systems (NEMS) and nano-optomechanical systems (NOMS).

Keywords : *First-principles calculations, ZnO monolayer, Band structure, Biaxial strains*

*E-mail: harihar@phy.iitb.ac.in; harihar@iopb.res.in

†Corresponding author's E-mail: gmukh@phy.iitb.ac.in; g.mukhopa@gmail.com

1 Introduction

Nanomaterials whose electronic properties can be controlled by mechanical strain are highly desirable for applications in nano-electromechanical systems (NEMS). If such materials happen to have direct band gaps, then those can find applications in nano-optomechanical systems (NOMS). If mechanical strain strongly affects the electronic properties of a material, then that material can be used as a strain sensor. Bulk ZnO, in its most stable wurtzite structure at ambient pressure, has many useful properties [1, 2] such as direct and wide band gap (E_g = 3.37 eV at room temperature and 3.44 eV at low temperatures), large exciton binding energy (60 meV), strong piezoelectric and pyroelectric properties, strong luminescence in the green-white region, large non-linear optical behavior, high thermal conductivity, radiation hardness, biocompatibility, and so on. These properties make ZnO an excellent candidate for a variety of applications in optics, electronics and photonics, sensors, transducers and actuators. Several ZnO nanostructures in the form of very thin nanosheets, nanowires, nanotubes and nanobelts have been synthesized and characterized using different preparation methods [3, 4]. In 2006, using the density functional theory (DFT) calculations, Freeman et al. [5] first predicted that when the layer number of ZnO films with (0001) orientation is small, the wurtzite structures are less stable than a phase based on 2D ZnO sheets with a layer ordering akin to that of hexagonal BN. In 2007, Tusche et al. [6] reported the observation of 2 monolayer (ML) thick ZnO(0001) films grown on Ag(111) by using surface X-ray diffraction and scanning tunneling microscopy. Very recently graphene-like honeycomb structures of ZnO have been prepared [7] on Pd(111) substrate. Theoretical studies [5,8–10] have now established the stability of the monolayer and few-layers (FL) of ZnO in planar honeycomb structures. This stability is attributed to the strong in-plane sp^2 hybridized bonds between the Zn and O atoms.

Recent theoretical studies on two dimensional (2D) flat ZnO nanostructures reported (i) the elastic, piezoelectric, electronic, and optical properties of ZnO monolayer (ML-ZnO) [10], (ii) room-temperature half-metallic ferromagnetism in the half-fluorinated ML-ZnO [11], (iii) fluorination induced half metallicity in few ZnO layers [12], (iv) fully-fluorinated and semi-fluorinated ZnO sheets [13] and (v) strain-induced semiconducting-metallic transition for ZnO zigzag nanoribbons [14]. Here, we report our DFT based investigation of the effect of homogeneous in-plane biaxial strain on the electronic properties of ML-ZnO - a specific study not found in the existing literature. This study simulates an experimental situation where ML-ZnO is supported on an ideal flat stretchable/flexible substrate.

2 Computational Methods

The calculations have been performed by using the DFT based full-potential (linearized) augmented plane wave plus local orbital (FP-(L)APW+lo) method [15] which is a descendant of FP-LAPW method [16]. We use the elk-code [17] and the Perdew-Zunger variant of LDA [18], the accuracy of which have been successfully tested in our previous works on graphene and silicene [19](silicon analog of graphene), germanene [20] (germanium analog of graphene)and graphene/h-BN heterobilayer [21]. The plane

wave cut-off of $|\mathbf{G}+\mathbf{k}|_{max} = 9.0/R_{mt}$ (a.u.$^{-1}$) (R_{mt} = the smallest muffin-tin radius) was chosen for plane wave expansion in the interstitial region. The Monkhorst-Pack [22] **k**-point grid size of $30 \times 30 \times 1$ was used for all calculations. The total energy was converged within 2μeV/atom. We simulate the 2D-hexagonal structure of ML-ZnO as a 3D-hexagonal supercell with a large value of c-parameter ($= |\mathbf{c}| = 40$ a.u.). The application of in-plane homogeneous biaxial strain δ up to $\pm 10\%$ was simulated by varying the in-plane lattice parameter $a(= |\mathbf{a}| = |\mathbf{b}|); \delta = (a - a_0)/a_0$, where a_0 is the ground state in-plane lattice constant. Figure 1 depicts the top-down view of a ML-ZnO in planar configuration.

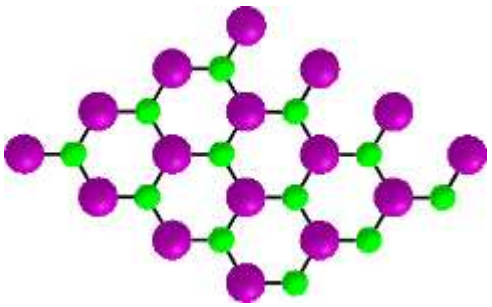

Figure 1: Top-down view of a ZnO monolayer in graphene-like honeycomb structure in ball-stick model. The large (pink) ball represents Zn atom and the small (green) ball represents the O atom.

3 Results and Discussions

Our calculated LDA value of $a_0 = 3.20$ Å corresponds to the Zn-O bond length $d_{Zn-O} = a_0/\sqrt{3} = 1.848$ Å, which is in agreement with the reported experimental [6] value of $d_{Zn-O} = 1.92$ Å and theoretical values of $d_{Zn-O} = 1.86$ Å by Tu and Hu [8], 1.895 Å by Topsakal et al. [9], 1.853 Å by Tu [10], 1.85 Å by Wang [12]. Our 3.75% underestimation of d_{Zn-O} value with respect to the experimental value is due to the well known problem of underestimation of the lattice constant within LDA. In our previous studies [18, 19] of graphene, silicene and germanene, we have demonstrated that the value of c-parameter chosen in the construction of supercell for simulation of 2D hexagonal structures also affects the value of in-plane lattice constant: larger value of c-parameter yields a slight smaller value of a. Since we use a different method and a different value of c-parameter, the disagreement of our result on a_0 with other theoretical result [9] is acceptable.

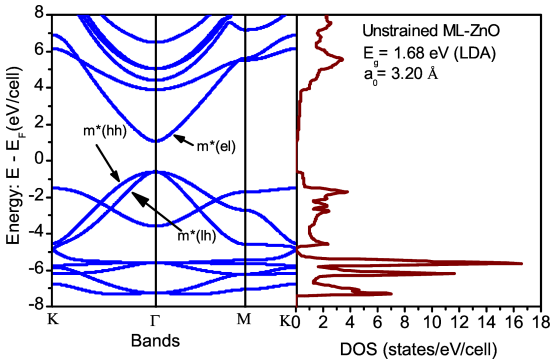

Figure 2: Bands and total DOS of unstrained ML-ZnO within LDA. E_F is the Fermi energy.

The electronic band structure and total density of states (DOS) plots of ML-ZnO are depicted in Figure 2. As seen in Figure 2, ML-ZnO is a direct band gap ($E_g = 1.68$ eV, LDA value) semiconductor with both valence band maximum (VBM) and conduction band minimum located at the Γ point of the hexagonal Brillouin Zone (BZ). However, the actual band gap is expected to be larger as LDA is known to underestimate the gap. Our calculated LDA band gap of 1.68 eV is in agreement with pre-

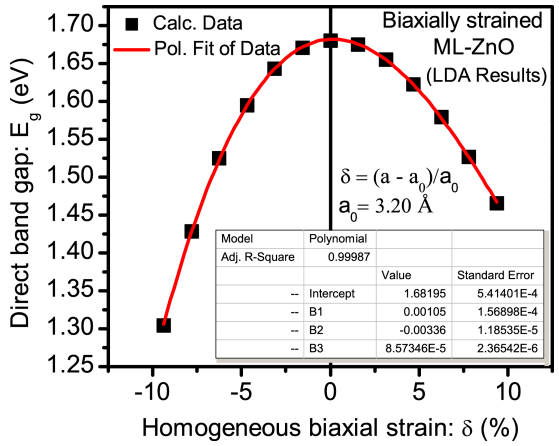

Figure 3: Variation of the direct band gap of ML-ZnO with in-plane homogeneous biaxial strain δ.

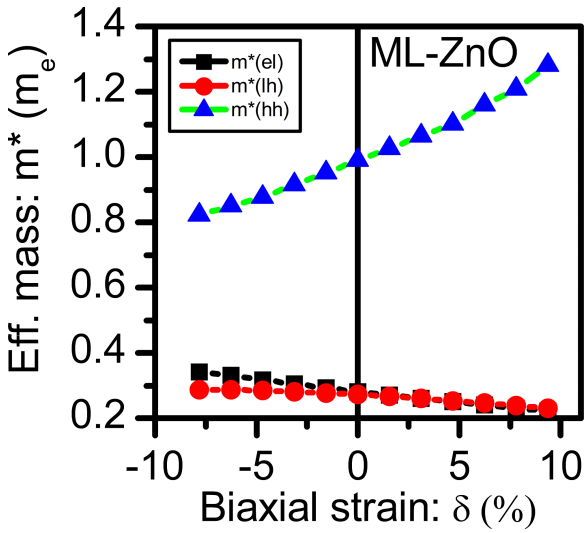

Figure 4: Variation of effective masses of the electron $m^{\star}$(el), light hole $m^{\star}$(lh) and heavy hole $m^{\star}$(hh) at the Γ point of the BZ with in-plane homogeneous biaxial strain.

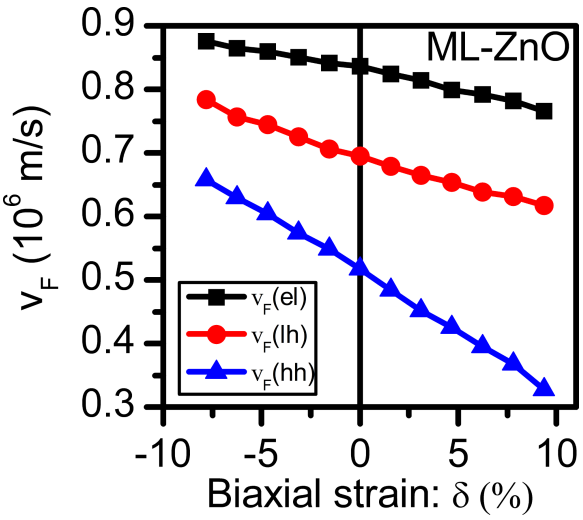

Figure 5: Variation of Fermi velocities of the electron v_F(el), light hole v_F(lh) and heavy hole v_F(hh) at the Γ point of the BZ with in-plane homogeneous biaxial strain.

vious calculations of 1.68 eV by Topsakal et al. [9], 1.762 eV by Tu [10], 1.84 eV by Wang et al. [13]. Using the GW approximations, recently Tu [10] estimated the direct band gap of ML-ZnO at 3.576 eV, which showed ML-ZnO as a wide band gap semiconductor. Although both LDA and generalized gradient approximations (GGA) do not yield the band gap correctly, these are powerful enough to predict the correct trend in variation of the gap [23–26]. Since we focus on the trend as well as the nature of variation in band gap (such as the possible transition from direct to indirect gap-phase as reported theoretically for uniaxially strained ZnO nanotubes [27] and ZnO nanowires and nanotubes [28]) rather than its absolute value, we employed the computationally simpler and less time-consuming LDA for investigating the effect of biaxial strain on band parameters of ML-ZnO.

Our calculated results on homogeneous biaxial strain-induced modifications of the band gap of ML-ZnO are depicted in Figure 3, which shows a strong non-linear variation of band gap with bi-

axial strain. Within our simulated strain limits ($\approx -10\% < \delta < 10\%$) as shown in Figure 3, the band gap E_g remains direct and its value varies with $\delta\,(= [(a - a_0)/a_0)] \times 100\,\%)$ as

$$E_g(\delta) = B_0 + B_1 \times \delta + B_2 \times \delta^2 + B_3 \times \delta^3 \quad (1)$$

where $B_0 = 1.68195$ eV, $B_1 = 0.00105$ eV, $B_2 = -0.00336$ eV, $B_3 = 8.57346 \times 10^{-5}$ eV, obtained by polynomial fit of our computed data. This may be useful in calculating the LDA band gap corresponding to a particular value of biaxial strain δ in the given range. Our prediction of strain-engineered band gap of ML-ZnO, if verified by experiments, may be useful in fabrication of NEMS and NOMS based on a graphene-analogue of ZnO. The energy bands very close to the $\Gamma-$point are parabolic, which enabled us to define and estimate the effective masses. Figure 4 depicts the nature of variation of effective masses of electrons $m^\star$(el), light holes $m^\star$(lh) and heavy holes $m^\star$(hh) at the Γ-point of the BZ (see Figure 2) with our simulated biaxial stain. Slightly away from the parabolic bands close to the $\Gamma-$point, the bands are linear in k which allowed us to calculate the Fermi velocity (v_F) values from their slopes. The nature of variation of our calculated Fermi velocities of electrons v_F(el), light holes v_F(lh) and the heavy holes v_F(hh) near the Γ-point of the BZ with our simulated biaxial stain is depicted in Figure 5. We found that the Fermi velocity v_F(el) of unstrained ML-ZnO (v_F(el) $= 0.836 \times 10^6$ m/s for $\delta = 0$ in Figure 5) near the Γ-point of BZ is close to he experimentally observed value of $v_F = 0.79 \times 10^6$ m/s in monolayer graphene (MLG) deposited on graphite substrate [29] and the theoretically calculated DFT value of $v_F = 0.833 \times 10^6$ m/s in MLG [30] and $v_F \simeq 0.8 \times 10^6$ m/s in MLG supported on monolayer of hexagonal boron nitride [21,31]. Since the charge carriers enter into ballistic transport limit when they have high velocities in the absence of scattering [32], we expect ballistic transport in ML-ZnO due to the high velocity of charge carriers analogous to the case of graphene.

4 Conclusions

Our all-electron full-potential density functional theory based calculations show that band-gap, effective masses and Fermi velocities of charge carriers in ML-ZnO in graphene-like honeycomb structure are mechanically tunable by application of in-plane homogeneous biaxial strain. Our predictions on strong non-linear variation of direct band gap with biaxial strain (Figure 3), non-linear increase of $m^\star$(el), and almost linear decrease in $m^\star$(lh) and $m^\star$(hh) with increasing strain (Figure 4) and almost linear decrease in the Fermi velocities of charge carriers with increasing strain (Figure 5) are not only novel but also experimentally testable by application of biaxial strain to a flat stretchable/flexible substrate supporting ML-ZnO. Our results are significant in that an analogous honeycomb-structure 'graphene' does not show any variations of its band gap under similar biaxial strains and currently a lot research is being done not only to open but also to control the band gap in graphene. Owing to its direct band gap with strong non-linear variation with biaxial strain, ML-ZnO should have potential applications in mechatronics/straintronics and other nano-devices such as the NEMS and NOMS.

References

[1] A. Janotti and C. G Van de Walle, Rep. Prog. Phys. 72 (2009) 126501.

[2] H. Morkoç and Ü. Özgür, Zinc Oxide: Fundamentals, Materials and Device Technology (WILEY-VCH Verlag GmbH & Co. KGaA, Weinheim, 2009).

[3] Z. L. Wang, ZnO Bulk, Thin Films and Nanostructures (Elsevier, Oxford, 2006).

[4] L. Schmidt-Mende and J. L. MacManus-Driscoll, Mater. Today 10 (2007) 40.

[5] C. L. Freeman, F. Claeyssens, N. L. Allan, and J. H. Harding, Phy. Rev. Lett. 96 (2006) 066102.

[6] C. Tusche, H. L. Meyerheim, J. Kirschner, Phys. Rev. Lett. 99 (2007) 026102.

[7] G. Weirrum, G. Barcaro, F. Fortunelli, F. Weber, R. Schennech, S. Surnev, F. Netzer, J. Phys. Chem. C 114 (2010) 15432.

[8] Z. C. Tu, X. Hu, Phys. Rev. B 74 (2006) 035434.

[9] M. Topsakal, S. Cahangirov, E. Bekaroglu, S. Ciraci, Phys. Rev. B 80 (2009) 235119.

[10] Z. C. Tu, J. Compu. Theor. Nanosci. 7 (2010) 1182; arXiv:0901.1112v3.

[11] E. J. Kan, H. J. Xiang, F. Wu, C. Tian, C. Lee, J. L. Yang, M.-H. Whangbo, Appl. Phys. Lett. 97 (2010) 122503.

[12] Q. Chen, J. Wang, L. Zhu, S. Wang, F. Ding, J. Chem. Phys. 132 (2010) 204703.

[13] Y. Wang, Y. Ding, J. Ni, S. Shi, C. Li, J. Shi, Appl. Phys. Lett. 96 (2010) 213117.

[14] H. Si, B. C. Pan, J. Appl. Phys. 107 (2010) 094313.

[15] E. Sjöstedt, L. Nordström, D.J. Singh, Solid State Commun. 114 (2000) 15.

[16] E. Wimmer, H. Krakauer, M. Weinert, J.A. Freeman, Phys. Rev. B 24 (1981) 864.

[17] Elk is an open source code: http://elk.sourceforge.net/

[18] J. P. Perdew, A. Zunger, Phys. Rev. B 23 (1981) 5048.

[19] H. Behera, G. Mukhopadhyay, AIP Conf. Proc. 1313 (2010), pp-152-155; arXiv:1111.1282.

[20] H. Behera, G. Mukhopadhyay, AIP Conf. Proc. 1349 (2011), pp-823-824; arXiv:1111.6333.

[21] H. Behera, G. Mukhopadhyay, J. Phys. Chem. Solids 73 (2012) 818; arXiv:1204.2030.

[22] H. J. Monkhorst, J. D. Pack, Phys. Rev. B 13 (1976) 5188.

[23] L. Dong, S. K. Yadav, R. Ramprasad, and S. P. Alpay, Appl. Phys. Lett. 96 (2010) 202106.

[24] Q. Chen, H. Hu, X. Chen, and J. Wang, Appl. Phys. Lett. 98 (2011) 053102.

[25] Y. W. Son, M. L. Cohen, and S. G. Louie, Nature 444 (2006) 347.

[26] D. K. Samarakoon and X. Q. Wang, ACS Nano 4 (2010) 4126.

[27] Y. Zhang, Y.-H. Wen, J.-C. Zheng, Z.-Z. Zhu, Phys. Lett. A 374 (2010) 2846.

[28] S. Li, Q. Jiang and G. W. Yang, Appl. Phys. Lett. 96 (2010) 213101.

[29] G. Li, A. Luican, and, E. Y. Andrei, Phys. Rev. Lett. 102 (2009) 176804.

[30] M. Gmitra, S. Konschuh, C. Ertler, C. Ambrosch-Draxl, and J. Fabian, Phys. Rev. B 80 (2009) 235431.

[31] Y. Fan, M. Zhao, Z.Wang, X.Zhang, H.Zhang, Appl. Phys. Lett. 98 (2011) 083103.

[32] S. Srisonphan, Y. S. Jung and H. K. Kim, Nature Nanotechnol. 7 (2012) 504.